Inorganic Chemistry

Article

pubs.acs.org/IC

Spin Exchange and Magnetic Dipole−Dipole Interactions Leading to the Magnetic Superstructures of MAs_2O_6 (M = Mn, Co, Ni)

Hyun-Joo Koo*[,†] and Myung-Hwan Whangbo*[,‡]

[†]Department of Chemistry and Research Institute for Basic Science, Kyung Hee University, Seoul 130-701, Republic of Korea

[‡]Department of Chemistry, North Carolina State University, Raleigh, North Carolina 27695-8204, United States

Supporting Information

ABSTRACT: The three isostructural magnetic oxides MAs_2O_6 (M = Mn, Co, Ni) containing high-spin M^{2+} ions undergo a long-range antiferromagnetic ordering below 30 K, but their ordered magnetic structures are not identical. While $CoAs_2O_6$ and $NiAs_2O_6$ adopt the commensurate superstructure of q_1 = (0, 0, 1/2), $MnAs_2O_6$ has the incommensurate superstructure of q_2 = (0.055, 0.389, 0.136). The cause for this difference was examined by calculating their spin exchange and magnetic dipole−dipole interaction energies. In $CoAs_2O_6$ and $NiAs_2O_6$, the strongest M−O···O−M spin exchange, J_1, dominates over other exchanges, hence leading to the q_1 superstructure. For $MnAs_2O_6$, the spin exchanges are not a deciding factor leading to its magnetic superstructure, being all weak and comparable in strengths, but the magnetic dipole−dipole interactions are.

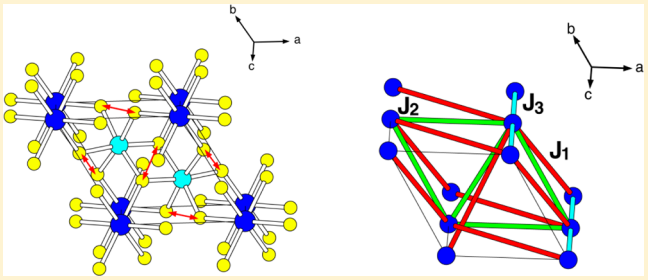

1. INTRODUCTION

The three transition-metal arsenates MAs_2O_6 (M = Mn, Co, Ni)[1] consist of the As_2O_6 honeycomb layers made up of edge-sharing AsO_6 octahedra (Figure 1a), which repeat along the *c*-direction such that the hexagonal rings of As^{5+} ions are eclipsed between two adjacent As_2O_6 layers. The high-spin M^{2+} ions occupy every O_6 octahedral site sandwiched between two adjacent hexagonal rings of As^{5+} ions along the *c*-direction (Figure 1b). The $MnAs_2O_6$, $CoAs_2O_6$, and $NiAs_2O_6$ arsenates exhibit a magnetic susceptibility maximum at $T_{max} \approx 13$, 20, and 30 K, respectively,[1] and their Curie−Weiss temperatures θ are −20.7, −64.4, and −66.2 K, respectively, indicating the presence of dominant antiferromagnetic (AFM) interactions in MAs_2O_6 (M = Mn, Co, Ni). $CoAs_2O_6$ and $NiAs_2O_6$ adopt a commensurate magnetic superstructure with propagation vector q_1 = (0, 0, 1/2), but $MnAs_2O_6$ adopts an incommensurate magnetic superstructure with q_2 = (0.055, 0.389, 0.136).[1] It is of interest to see why $CoAs_2O_6$ and $NiAs_2O_6$ differ from $MnAs_2O_6$ in their ordered magnetic structures. In general, the ordered magnetic structure of a magnetic compound is determined by spin exchange interactions, magneto-crystalline anisotropy (MCA) energies, and magnetic dipole−dipole (MDD) interactions.[2] The spin exchanges of MAs_2O_6 (M = Mn, Co, Ni) occur through the M−O···O−M exchange paths between adjacent M^{2+} ion sites (Figure 1c). It is now well-established that M−O···O−M exchange interactions can be much stronger than the M−O−M exchange interactions.[3,4] The present work is aimed at understanding why $CoAs_2O_6$ and $Ni_2As_2O_6$ adopt a commensurate superstructure q_1 but $MnAs_2O_6$ does not and what controls the incommensurate superstructure q_2 of $MnAs_2O_6$. For this purpose, we evaluate the three M−O···O−M exchange interactions of MAs_2O_6, depicted in Figure 1c, by performing energy-mapping analysis[2,3] based on density functional theory (DFT) calculations and also by carrying out magnetic MDD energy calculations.[5]

2. COMPUTATIONAL DETAILS

In our DFT electronic structure calculations for MAs_2O_6 (M = Mn, Co, Ni), we employed the projected augmented-wave (PAW) method encoded in the Vienna ab initio simulation package,[6] and the generalized gradient approximation (GGA) of Perdew, Burke, and Ernzerhof[7] for the exchange-correlation corrections, the plane wave cutoff energy of 400 eV, and the threshold of self-consistent field (SCF) energy convergence of 10^{-6} eV. The irreducible Brillouin zone was sampled with 54 k. To describe the electron correlation associated with the 3d states of Mn, Co, and Ni, the DFT plus on-site repulsion U (DFT+U)[8] calculations were carried out with effective $U_{eff} = U - J$ = 2, 3, and 4 eV on the Mn, Co, and Ni atoms. The MCA energy of the Mn^{2+} ion of $MnAs_2O_6$ was calculated by performing DFT+U calculations including spin−orbit coupling (SOC) with SCF energy convergence of 10^{-8} eV.

3. SPIN EXCHANGE INTERACTIONS AND MAGNETIC SUPERSTRUCTURES

The three spin exchange parameters J_1, J_2, and J_3 of MAs_2O_6 (M = Mn, Co, Ni) to be considered are depicted in Figure 1c, and the geometrical parameters associated with these paths are summarized in Table 1. Notice that, on going from Mn to Co to Ni, the M−O bond length decreases while increasing the

Received: January 22, 2014
Published: March 6, 2014

   dx.doi.org/10.1021/ic500156e | *Inorg. Chem.* 2014, 53, 3812−3817

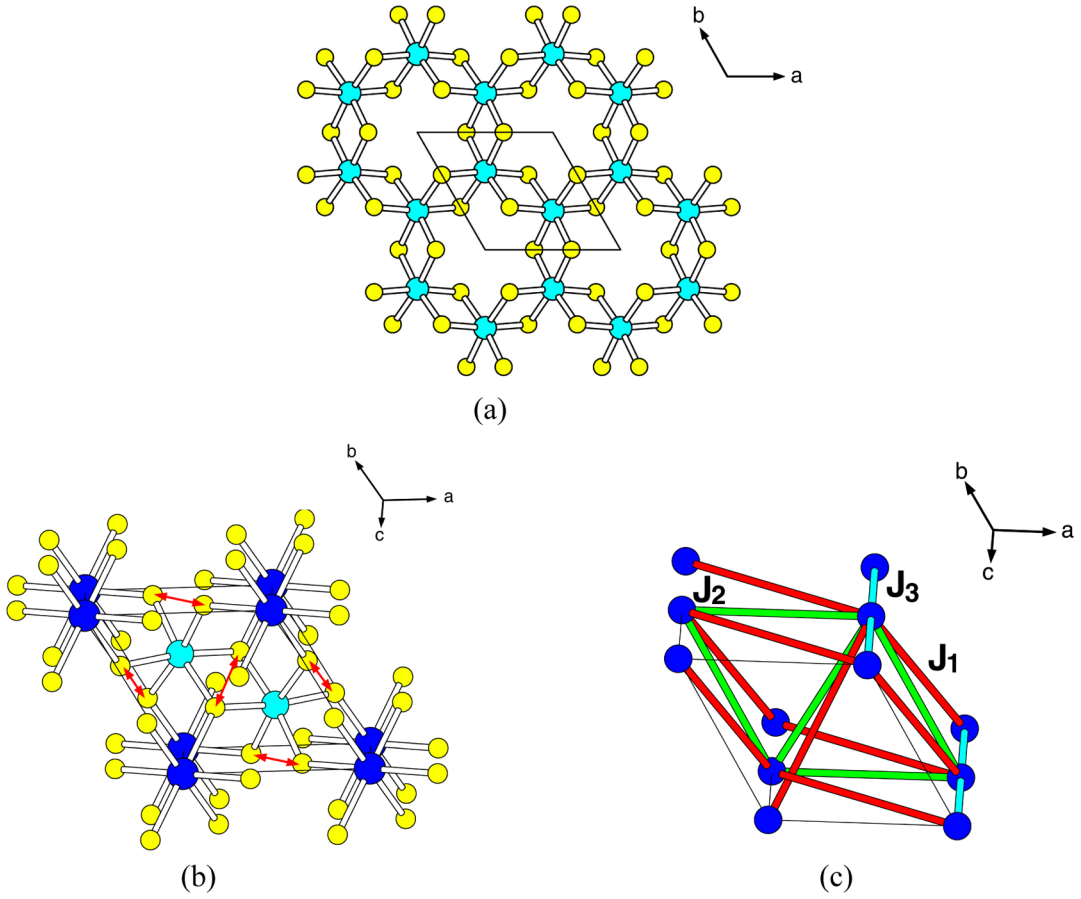

Figure 1. (a) As_2O_6 layer made up of edge-sharing AsO_6 octahedra. (b) Perspective view of crystal structure of MAs_2O_6 (M = Mn, Co, Ni), where the blue, cyan, and yellow circles represent M, As, and O atoms, respectively. The red arrows indicate the shortest O···O contacts in MAs_2O_6. (c) Spin exchange paths in MAs_2O_6 (M = Mn, Co, Ni), where the red, green, and cyan cylinders represent the spin change paths, J_1, J_2, and J_3, respectively.

Table 1. Geometrical Parameters Associated with the M−O···O−M Spin Exchange Paths in MAs_2O_6 (M = Mn, Co, Ni)

MAs_2O_6	M−O	O···O[a]	∠M—O···O[b]
M = Mn			
J_1	2.219	2.382	158.3
J_2		2.628	130.5, 85.3
J_3		2.699	100.8
M = Co			
J_1	2.131	2.405	158.7
J_2		2.645	132.0, 86.3
J_3		2.658	100.2
M = Ni			
J_1	2.098	2.410	159.1
J_2		2.646	132.5, 86.7
J_3		2.636	100.1

[a]The bond distances are in the unit of Å. [b]The bond angles are in the unit of degrees.

O···O contact distance of the J_1 path. To determine the J_1−J_3 values by energy-mapping analysis, we consider four ordered spin states FM, AF1, AF2, and AF3 presented in Figure 2. The energies of these states can be expressed in terms of the spin Hamiltonian

$$\hat{H} = -\sum_{i<j} J_{ij}\hat{S}_i\cdot\hat{S}_j \quad (1)$$

where $J_{ij} = J_1$, J_2, or J_3 is the spin exchange parameter for the interaction between the spin sites i and j. By applying the energy expression obtained for spin dimers with N unpaired spins per spin sites (N = 5, 3, and 2 for M = Mn, Co and Ni, respectively),[9] the total spin exchange energies per (2a, 2b, 2c) supercell, that is, per eight formula units (FUs) of the FM, AF1, AF2, and AF3 states can be written as

$$E = (n_1J_1 + n_2J_2 + n_3J_3)(N^2/4) \quad (2)$$

The coefficients n_1, n_2, and n_3 for the four spin ordered states are summarized in Figure 2. The relative energies of the FM, AF1, AF2, and AF3 states can also be calculated on the basis of DFT+U electronic structure calculations, which are summarized in Table S1 of the Supporting Information. Our DFT+U calculations show that the AF1 state is the most stable state for all the MAs_2O_6 (M = Mn, Co, Ni) arsenates. By mapping the energy differences between the ordered spin states obtained from the DFT+U calculations onto the corresponding energy differences obtained from the spin Hamiltonian, we obtain the values of J_1, J_2, and J_3, which are summarized in Table 2.

In MAs_2O_6 (M = Mn, Co, Ni), J_1 is AFM and is the dominant one for all the U_{eff} values employed. The values of J_2 and J_3 are negligible compared to J_1 in $Co_2As_2O_6$ and $NiAs_2O_6$. However, for $MnAs_2O_6$, J_1 is weak and is comparable in magnitude to the J_2 and J_3 values. It is noteworthy that the strength of J_1 increases in the order of $MnAs_2O_6$ < $CoAs_2O_6$ < $NiAs_2O_6$ (Table 2), despite the O···O contact distance of the

dx.doi.org/10.1021/ic500156e | Inorg. Chem. 2014, 53, 3812−3817

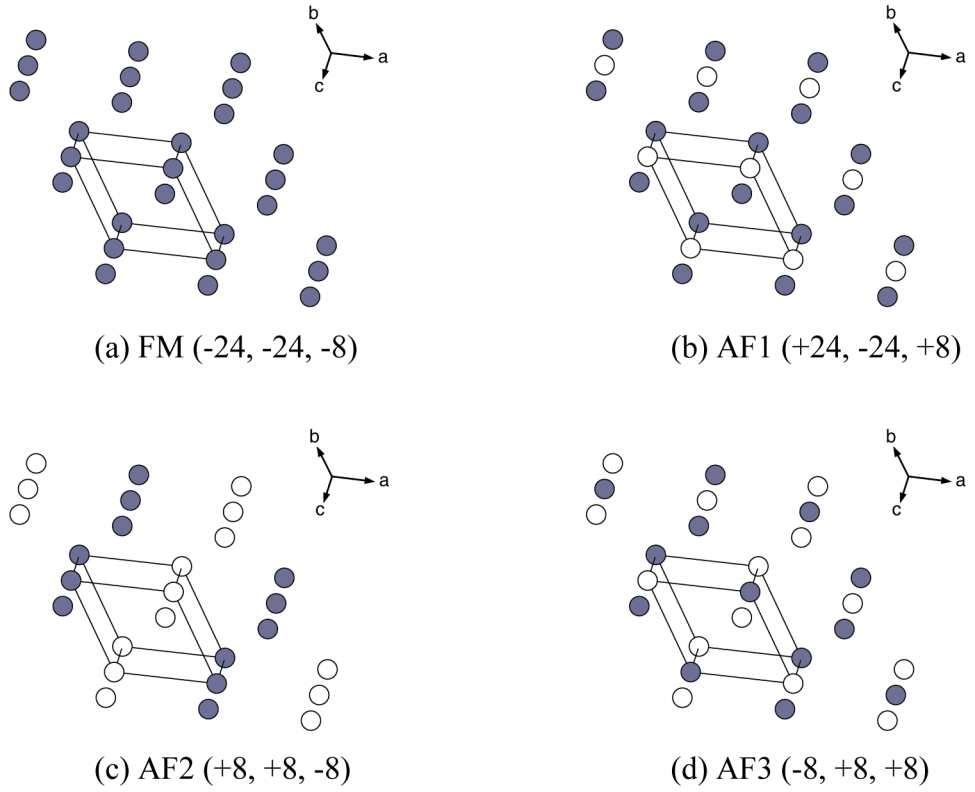

Figure 2. Ordered spin arrangements of the (a) FM, (b) AF1, (c) AF2, and (d) AF3 states of MAs_2O_6 (M = Mn, Co, Ni), where the gray and white circles represent the up and down spin sites of M^{2+} ions. The numbers in the parentheses for each state show the coefficients n_1, n_2, and n_3 of eq 2 for that state.

Table 2. Spin Exchange Parameters (in K) and the Curie–Weiss Temperature (in K) of MAs_2O_6 (M = Mn, Co, Ni) Obtained from DFT+U Calculations

(a) $MnAs_2O_6$			
U_{eff}	2 eV	3 eV	4 eV
J_1/k_B	−1.8	−1.3	−1.0
J_2/k_B	−0.9	−0.7	−0.6
J_3/k_B	−0.6	−0.4	−0.3
θ	−50.1	−38.0	−29.2
(b) $CoAs_2O_6$			
U_{eff}	2 eV	3 eV	4 eV
J_1/k_B	−11.7	−8.9	−6.8
J_2/k_B	−0.1	−0.2	−0.2
J_3/k_B	−0.4	−0.4	−0.3
θ	−88.9	−68.8	−53.0
(c) $NiAs_2O_6$			
U_{eff}	2 eV	3 eV	4 eV
J_1/k_B	−31.4	−24.2	−18.6
J_2/k_B	−0.1	−0.1	−0.1
J_3/k_B	+1.7	+1.2	+0.8
θ	−123.4	−95.6	−73.8

associated M–O···O–M exchange path increasing in the same order. This counterintuitive observation reflects the fact that the electronegativity of M increases in the order of Mn < Co < Ni, so the energy difference Δe between the M 3d and the O 2p orbitals decreases in the order of Mn > Co > Ni. The d-block orbitals (namely, the t_{2g} and e_g orbitals) of an MO_6 octahedron, in which the M 3d orbitals are combined out-of-phase with the O 2s/2p orbitals, have a greater weight on the O 2p orbitals with decreasing Δe.[10] To illustrate this point, the d-block orbitals of the MnO_6 and NiO_6 octahedra, taken from $MnAs_2O_6$ and $NiAs_2O_6$, respectively, were determined by performing extended Hückel tight-binding calculations.[11] For simplicity, only the x^2-y^2 orbital (one of the e_g orbitals) of the MnO_6 octahedron is compared with that of the NiO_6 octahedron in Figure 3, which shows clearly that the weight of the O 2s/2p orbitals in the x^2-y^2 orbital is greater in the NiO_6 than it is in the MnO_6 octahedron. As the weight on the O 2p orbital is increased, the overlap between two magnetic orbitals (namely, singly filled 3d-block orbitals) of the M–O···O–M exchange path J_1 will increase through the O···O contact (Figure 4), hence leading to a stronger AFM spin exchange.[2,3] This overcomes the effect of slightly increasing the O···O contact distance in the J_1 path.

To see how reasonable the calculated values of J_1, J_2, and J_3 are, we estimate the Curie–Weiss temperature θ in terms of these parameters. In the mean-field theory,[12] which is valid in the paramagnetic limit, θ is related to the spin exchange parameters as follows:

$$\theta = \frac{S(S+1)}{3k_B}\sum_i z_i J_i \qquad (3)$$

where the summation runs over all nearest neighbors of a given spin site, z_i is the number of nearest neighbors connected by the spin exchange parameters J_i, and S is the spin quantum number of each spin site (i.e., S = 5/2, 3/2, and 1 for Mn, Co, and Ni, respectively). The evaluated Curie–Weiss temperatures θ, using the J values obtained from DFT+U calculations, are summarized in Table 2. The calculated θ values are in good

dx.doi.org/10.1021/ic500156e | Inorg. Chem. 2014, 53, 3812–3817

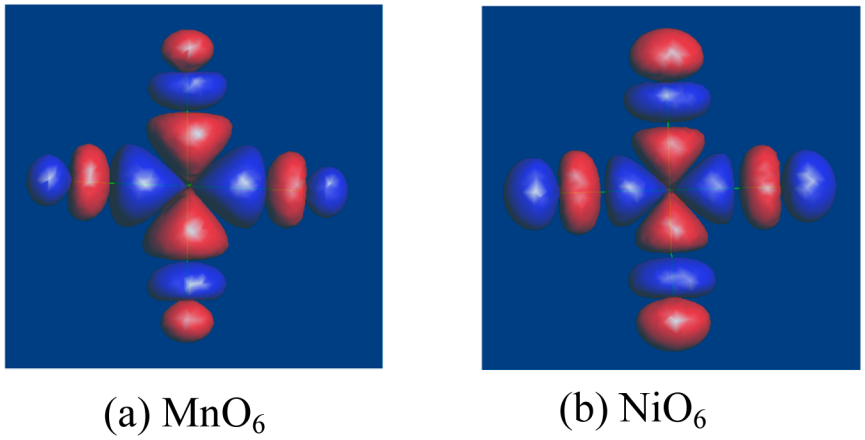

Figure 3. Comparison of the x^2-y^2 orbitals of the MnO_6 and NiO_6 octahedra present in $MnAs_2O_6$ and $NiAs_2O_6$, respectively, determined from extended Hückel tight-binding calculations.

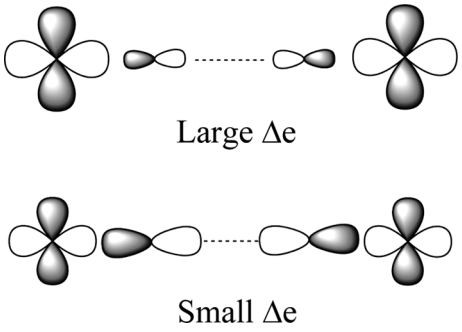

Figure 4. Effect of the energy difference Δe between the M 3d and O 2p orbitals on the weight of the 2p orbital in the d-block levels of an MO_6 octahedron. For simplicity, only one M−O bond of the σ^* orbital is depicted.

agreement with those from experiments, when U_{eff} = 4, 3, and 4 eV for $MnAs_2O_6$, $CoAs_2O_6$, and $NiAs_2O_6$, respectively.

Let us now examine the reason why $CoAs_2O_6$ and $NiAs_2O_6$ adopt a magnetic superstructure q_1 = (0, 0, 1/2), but $MnAs_2O_6$ adopts a magnetic superstructure with q_2 = (0.055, 0.389, 0.136). We approximate the q_2 incommensurate superstructure by the commensurate ones q_3 = (0, 1/3, 0) and q_4 = (0, 1/3, 1/7). The ordered spin arrangements leading to the q_1 and q_3 superstructures are presented in Figure 5a and 5b, respectively, and those leading to the q_4 superstructure appear in Figure 6. The energies of the q_1, q_3, and q_4 superstructures per FU are expressed in terms of J_1−J_3 as follows:

$$E(q_1) = (3J_1 - 3J_2 + J_3)(N^2/4)$$

$$E(q_3) = (-J_1/3 - J_2/3 - J_3)(N^2/4)$$

$$E(q_4) = (-J_1/7 - J_2/3 - 3J_3/7)(N^2/4) \quad (4)$$

Note that the six different spin arrangements of Figure 6 for the q_4 structure have the same energy. The energies $E(q_1)$, $E(q_3)$, and $E(q_4)$ calculated for MAs_2O_6 (M = Mn, Co, Ni) are summarized in Table 3. For all MAs_2O_6 (M = Mn, Co, Ni), the q_4 superstructure is slightly lower in energy than is the q_3 superstructure. For $CoAs_2O_6$ and $NiAs_2O_6$, the q_1 superstructure is much more stable than the q_3 and q_4 superstructures. This is because their J_1 exchange is much stronger than their J_2 and J_3 exchanges and explains why they adopt the q_1 superstructure. $MnAs_2O_6$ is much less stable than $CoAs_2O_6$ and $NiAs_2O_6$ in the q_1 superstructure, but is comparable in energy with $CoAs_2O_6$ and $NiAs_2O_6$ in the q_3 and q_4 superstructures. For $MnAs_2O_6$, however, the q_1, q_3, and q_4 superstructures are essentially similar in energy, suggesting that its spin exchange interactions are not a major factor affecting its magnetic superstructure. In essence, $MnAs_2O_6$ differs in magnetic superstructure from $CoAs_2O_6$ and $NiAs_2O_6$ because its spin exchanges J_1, J_2, and J_3 are weak and comparable in magnitude, whereas J_1 is much stronger than J_2 and J_3 in $Co_2As_2O_6$ and $NiAs_2O_6$.

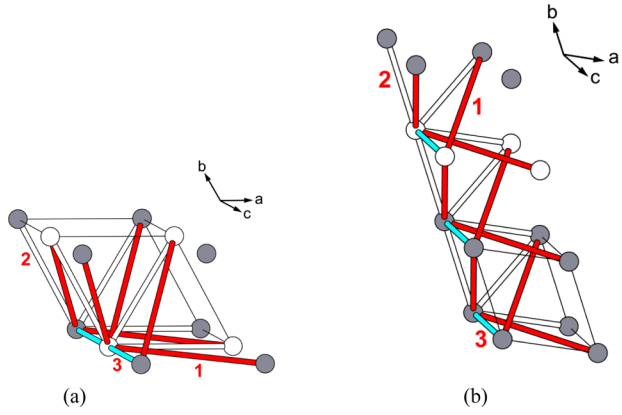

Figure 5. Magnetic cells of (a) q_1 = (0, 0, 1/2) and (b) q_3 = (0, 1/3, 0) superstructures. Here the gray and white spheres represent the up-spin and down-spin of M^{2+} ions, respectively. The numbers 1, 2, and 3 represent the spin exchange paths J_1, J_2, and J_3, respectively.

4. MAGNETIC DIPOLE−DIPOLE INTERACTIONS AND MAGNETIC SUPERSTRUCTURES

We now examine if MDD interactions[5] contribute to the magnetic superstructures of MAs_2O_6 (M = Mn, Co, Ni) since, though weak, they were found to be responsible for the spin orientation and long-range antiferromagnetic ordering of $Sr_3Fe_2O_5$,[5] Ni_3TeO_6,[13] and Cs_2AgF_4.[14] Given that two spins located at sites i and j are described by the distance r_{ij} with the unit vector $\vec{e}_{ij}$ along the distance, the MDD interaction is described by[5]

$$\left(\frac{g^2\mu_B^2}{a_0^3}\right)\left(\frac{a_0}{r_{ij}}\right)^3 [-3(\vec{S}_i\cdot\vec{e}_{ij})(\vec{S}_j\cdot\vec{e}_{ij}) + (\vec{S}_i\cdot\vec{S}_j)] \quad (5)$$

dx.doi.org/10.1021/ic500156e | Inorg. Chem. 2014, 53, 3812−3817

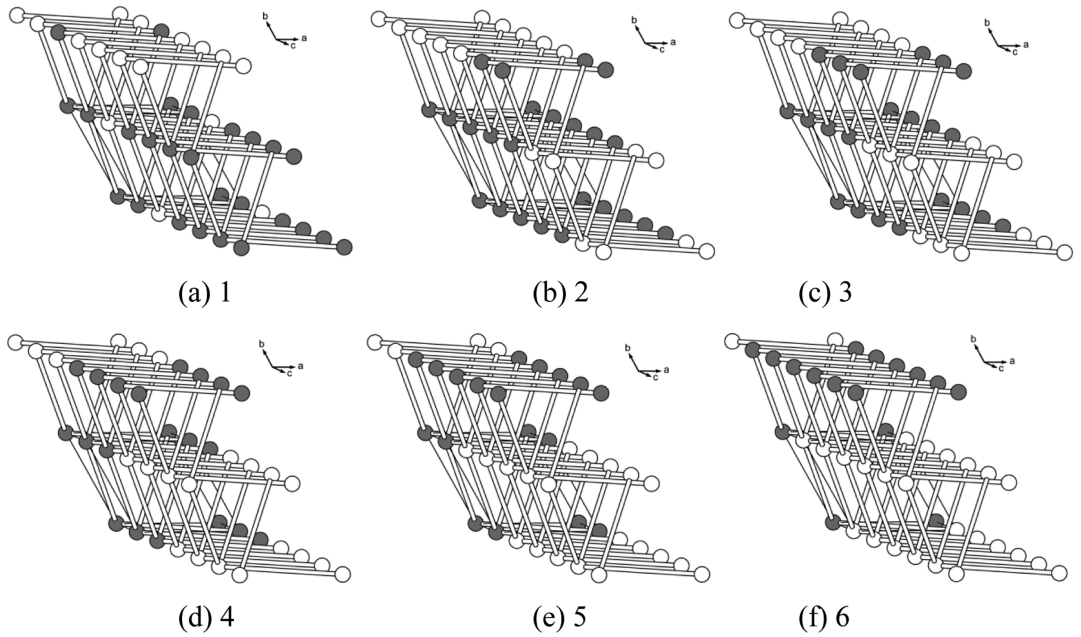

Figure 6. Six spin arrangements leading to the magnetic superstructure $q_4 = (0, 1/3, 1/7)$. Here the gray and white spheres represent the up-spin and down-spin of M^{2+} ions, respectively, and the white cylinders represent the J_1 paths.

Table 3. Spin Exchange Energies (in K/FU) of the q_1, q_3, and q_4 Magnetic Superstructures of MAs_2O_6 (M = Mn, Co, Ni) Evaluated with the J/k_B (in K) Parameters Obtained from the DFT+U Calculations with U_{eff} (in eV)

	U_{eff}	J_1/k_B	J_2/k_B	J_3/k_B	$E(q_1)$	$E(q_3)$	$E(q_4)$
Mn	4	−1.0	−0.6	−0.3	−5.6	5.2	2.9
Co	3	−8.9	−0.2	−0.4	−57.8	7.9	3.4
Ni	4	−18.6	−0.1	0.8	−56.4	5.4	2.4

where a_0 is the Bohr radius (0.529177 Å) and $(g\mu_B)^2/(a_0)^3$ = 0.725 meV. In summing the MDD interactions between various pairs of spin sites, we employed the Ewald summation method.[15] The MDD interaction energies were calculated for the two magnetic superstructures $q_1 = (0, 0, 1/2)$ and $q_4 = (0, 1/3, 1/7)$ of $MnAs_2O_6$, using the Ewald summation method.

For the spin orientations at each spin site in the q_1 and q_4 superstructures, we consider the spin orientations parallel to the *a*- and *c*-directions ($\|a$ and $\|c$ directions, respectively). The MDD interaction energies calculated for the q_1 and q_4 superstructures of MAs_2O_6 (M = Mn, Co, Ni) are summarized in Table 4. For $CoAs_2O_6$ and $NiAs_2O_6$, the MDD interactions are very weak compared to the spin exchange interactions, so their adoption of the q_1 superstructure is determined by the spin exchanges. However, for $MnAs_2O_6$ with the $\|a$ spin orientation, the q_1 and q_4 superstructures, almost equal in stability, become energetically favorable structures. Since there are many more spin configurations leading to q_4 than to q_1, the adoption of the superstructure q_4 would be more favorable for $MnAs_2O_6$ in terms of MDD interactions.

Our discussion presented above for $MnAs_2O_6$ is hardly affected by the MCA of the Mn^{2+} ion because, according to our DFT+U+SOC calculations, the MCA is negligible; the $\|a$ spin orientation is preferred to the $\|c$ spin orientation only by 0.06 K per Mn^{2+} ion. This is not surprising because a high-spin Mn^{2+} ion is an $L = 0$ ion, so the SOC is expected to be negligible.

Table 4. MDD Interactions Energies (in K/FU) Calculated for the (0, 0, 1/2) and (0, 1/3, 1/7) Superstructures of MAs_2O_6 (M = Mn, Co, Ni)

(a) $q_1 = (0, 0, 1/2)$ superstructure			
spin	Mn	Co	Ni
$\|a$	−0.204	−0.075	−0.034
$\|c$	0.408	0.151	0.068

(b) $q_4 = (0, 1/3, 1/7)$ superstructure				
spin	config.	Mn	Co	Ni
$\|a$	1	−0.146	−0.052	−0.024
	2	−0.152	−0.055	−0.025
	3	−0.156	−0.056	−0.025
	4	−0.156	−0.056	−0.025
	5	−0.152	−0.055	−0.025
	6	−0.146	−0.052	−0.024
$\|c$	1	−0.055	−0.023	−0.011
	2	−0.036	−0.016	−0.007
	3	−0.029	−0.013	−0.006
	4	−0.029	−0.013	−0.006
	5	−0.036	−0.016	−0.007
	6	−0.055	−0.023	−0.011

5. CONCLUDING REMARKS

The strongest M−O···O−M spin exchange interactions J_1 of MAs_2O_6 (M = Mn, Co, Ni) decrease their strength in the order of $NiAs_2O_6$ > $CoAs_2O_6$ > $MnAs_2O_6$ because the O 2p contributions to the d-block levels of the MO_6 (M = Mn, Co, Ni) octahedra decrease in the order of NiO_6 > CoO_6 > MnO_6. $CoAs_2O_6$ and $NiAs_2O_6$ adopt the (0, 0, 1/2) superstructure because their spin exchanges are dominated by the strongest M−O···O−M spin exchange J_1. In $MnAs_2O_6$, all spin exchanges are weak and comparable in strength. Our analysis of its incommensurate superstructure (0.055, 0.389, 0.136), using the commensurate approximation (0, 1/3, 1/7), indicates that the spin exchange interactions are not a deciding factor leading to

dx.doi.org/10.1021/ic500156e | Inorg. Chem. 2014, 53, 3812−3817

the superstructure, but the magnetic dipole−dipole interactions are.

■ ASSOCIATED CONTENT

Supporting Information

Table S1, showing relative energies of ordered spin states of MAs_2O_6, obtained from DFT calculations, is available free of charge via the Internet at http://pubs.acs.org.

■ AUTHOR INFORMATION

Corresponding Authors

*H.-J. K.: hjkoo@khu.ac.kr.

*M.-H.W.: mike_whangbo@ncsu.edu.

Notes

The authors declare no competing financial interest.

■ ACKNOWLEDGMENTS

This research was supported by Basic Science Research Program through the National Research Foundation of Korea (NRF) funded by the Ministry of Education, Science and Technology (2010-0021042) and by the computing resources of the NERSC Center and the HPC Center of NCSU.

■ REFERENCES

(1) Nakua, A. M.; Greedan, J. E. *J. Solid State Chem.* **1995**, *118*, 402−411.

(2) Xiang, H. J.; Lee, C.; Koo, H.-J.; Gong, X. G.; Whangbo, M.-H. *Dalton Trans.* **2013**, *42*, 823−853 and the references cited thererin.

(3) Whangbo, M.-H.; Koo, H.-J.; Dai, D. *J. Solid State Chem.* **2003**, *176*, 417−481 and the references cited thererin.

(4) (a) Koo, H.-J.; Whangbo, M.-H. *Inorg. Chem.* **2001**, *40*, 2161−2169. (b) Koo, H.-J.; Whangbo, M.-H.; VerNooy, P. D.; Torardi, C. C.; Marshall, W. J. *Inorg. Chem.* **2002**, *41*, 4664−4672. (c) Whangbo, M.-H.; Koo, H.-J.; Dai, D.; Jung, D. *Inorg. Chem.* **2003**, *42*, 3898−3906. (d) Koo, H.-J.; Whangbo, M.-H.; Lee, K.-S. *Inorg. Chem.* **2003**, *42*, 5932−5937. (e) Dai, D.; Koo, H.-J.; Whangbo, M.-H. *Inorg. Chem.* **2004**, *43*, 4026−4035. (f) Koo, H.-J.; Dai, D.; Whangbo, M.-H. *Inorg. Chem.* **2005**, *44*, 4359−4365.

(5) Koo, H.-J.; Xiang, H. J.; Lee, C.; Whangbo, M.-H. *Inorg. Chem.* **2009**, *48*, 9051−9053.

(6) (a) Kresse, G.; Hafner, J. *Phys. Rev. B* **1993**, *47*, 558−561. (b) Kresse, G.; Furthmüller, J. *Comput. Mater. Sci.* **1996**, *6*, 15−50. (c) Kresse, G.; Furthmüller, J. *Phys. Rev. B* **1996**, *54*, 11169−11186.

(7) Perdew, J. P.; Burke, S.; Ernzerhof, M. *Phys. Rev. Lett.* **1996**, *77*, 3865−3868.

(8) Dudarev, S. L.; Botton, G. A.; Savrasov, S. Y.; Humphreys, C. J.; Sutton, A. P. *Phys. Rev. B* **1998**, *57*, 1505−1509.

(9) (a) Dai, D.; Whangbo, M.-H. *J. Chem. Phys.* **2001**, *114*, 2887−2893. (b) Dai, D.; Whangbo, M.-H. *J. Chem. Phys.* **2003**, *118*, 29−39.

(10) Albright, T. A.; Burdett, J. K.; Whangbo, M.-H. *Orbital Interactions in Chemistry*, 2nd ed.; Wiley: New York, 2013.

(11) (a) Hoffmann, R. *J. Chem. Phys.* **1963**, *39*, 1397−1412. (b) Our calculations were carried out by employing the SAMOA (Structure and Molecular Orbital Analyzer) program package. This program can be downloaded free of charge from the Web site http://primec.com/products.htm.

(12) Smart, J. S. *Effective Field Theory of Magnetism;* Saunders: Philadelphia, 1966.

(13) Wu, F.; Kan, E. J.; Tian, C.; Whangbo, M.-H. *Inorg. Chem.* **2010**, *49*, 7545−7548.

(14) Tong, J.; Kremer, R. K.; Köhler, J.; Simon, I. A.; Lee, C.; Kan, E.; Whangbo, M.-H. *Z. Kristallogr.* **2010**, *225*, 498−503.

(15) (a) Ewald, P. P. *Ann. Phys.* **1921**, *64*, 253−287. (b) Darden, T.; York, D.; Pedersen, L. *J. Chem. Phys.* **1993**, *98*, 10089−10092. (c) Wang, H.; Dommert, F.; Holm, C. *J. Chem. Phys.* **2010**, *133*, 034117.